Research Article
Volume 16:06, 2024

Journal of Cancer Science and Therapy

ISSN: 1948-5956 Open Access

Use of Pixel Intensity Measurements Derived from OCT Images to Differentiate Between Seborrheic Keratosis and Melanomas: A Pilot Study

Frederick H. Silver[1,2*], Tanmay Deshmukh[2], Aanal Patel[1] and Hari Nadaminti[3]

[1]Department of Pathology and Laboratory Medicine, Robert Wood Johnson Medical School, Rutgers, The State University of New Jersey, New Brunswick, NJ 08854, USA
[2]OptoVibronex, LLC. Ben Franklin Tech Ventures, Bethlehem, PA 18105, USA
[3]Summit Health, Dermatology, Berkeley Heights, NJ 07922, USA

Abstract

Differentiating Seborrheic Keratosis (SK) from melanoma can be difficult based on visual observations and dermoscopy since both are pigmented lesions. While SK is considered a benign lesion that is localized, in contrast melanoma can spread to other tissues and lead to death if it metastasizes. Therefore, it is important to be able to noninvasively differentiate between SK and melanoma to limit the number of unnecessary biopsies performed. We have measured the pixel intensity of Optical Coherence Tomography (OCT) images of normal skin, SK, and melanoma by breaking OCT images into low (green), medium (blue) and high (red) pixel intensity vs. depth images. Normal skin and SK are characterized by higher green scale pixel intensity vs. depth plots while melanoma has a lower green scale pixel intensity vs. depth plot. Melanoma also has lower red scale pixel intensity vs. depth plot compared to SK and normal skin. Our results show that a decreased pixel intensity of the superficial epidermis that is observed in melanomas is likely due to formation of melanin aggregates that approach the wavelength of light in size. The decreased pixel intensity of melanoma is likely a result of increased amounts of melanin particles in melanocytes and keratinocytes. The specificity and sensitivity of differentiating SK and melanoma and normal skin from melanoma based on quantitative pixel intensity vs. depth are about 85% to 100%, respectively. The sensitivity and specificity of differentiating normal skin from SK is 60% and 100%, respectively. These results suggest that color-coded OCT images can be used to noninvasively screen for melanomas along with dermoscopy and visual inspection. The ability to collect OCT lesion data noninvasively in concert with remote data acquisition will allow rapid patient screening for melanomas in areas where dermatologist visits are difficult to schedule.

Keywords: Optical coherence tomography • Pixel intensity • Melanoma • Seborrheic keratosis • Dermoscopy • Visual inspection

Introduction

Cutaneous Melanoma (CM) is a malignancy arising particularly in white populations [1]. It is related to UV light exposure from direct exposure to sunlight and indoor tanning beds. Changes in sunbathing habits leading to more ultraviolet radiation exposure and an increasing use of indoor tanning beds play a central role in the rise of CM that has been reported from all Caucasian populations studied [1-3]. CM is typically a highly visible cancer due to the presence of varying amounts of brown pigment. The incidence of CM has been rising rapidly in many populations and melanoma survival is correlated with tumor thickness [1-3]. Therefore, early detection is a strategy for reducing the incidence of malignant melanoma. CM is a particularly aggressive form of cancer that originates from melanocytes, the pigment-producing cells derived from the neural crest [4,5]. Despite representing a mere 4% of all skin cancers, CM accounts for up to 75% of skin cancer-related deaths [5]. However, with early detection and proper intervention, over 90% of the cases can be cured [4]. The global estimate of new melanoma cases and deaths is about 325,000, and 57,000, respectively [5-7]. If the rates remain stable, the global burden from melanoma is estimated to increase to 510,000 new cases and 96,000 deaths by 2040 [6].

Despite the increasing number of global melanoma cases, many deaths can be averted through effective prevention, early detection, and effective curative treatments [7]. In Italy, the increasing CM incidence trend is reported to be accurate [8] and increased patient presentation at dermatologic offices has led to increased number of biopsies [8]. Tumor thickness appears to be the most important factor for prediction of malignancy [9]. The survival of patients with melanoma were not consistently associated with mitotic activity. High mitotic activity was generally associated with thick lesions and poor prognosis [9]. One diagnostic problem is that other pigmented lesions including seborrheic keratosis and pigmented basal cell carcinoma can be misdiagnosed as melanomas. Seborrheic Keratosis (SK) is one of the most common epidermal tumors that affects both sexes equally, and usually arises in individuals older than 50 years [10]. It can be similar in gross morphology to melanoma [10]. The tumor may become cancerous in a small fraction of cases [11]. While most dermatologists can identify SK lesions it is sometimes difficult to differentiate between inflammed SK and melanoma [12]. Dermoscopy improves the diagnosis of benign and malignant cutaneous neoplasms in comparison with examination with the unaided eye and should be used routinely for all pigmented and non-pigmented cutaneous neoplasms [12].

Optical Coherence Tomography (OCT) has also been used to identify skin cancers. OCT is an imaging technique that applies infrared light to the skin, which allows light to penetrate without causing tissue changes [13-16]. It is used in dermatology for evaluation of benign and cancerous lesions [16]. OCT uses infrared light reflected from the different components of surface tissues to generate an image. It provides cross-sectional and volume scans of skin at depths between 0.4 and 2.0 m with resolution between 3 and 15 micrometers [13-16]. OCT provides quick and useful diagnostic images for several clinical problems and is a valuable addition or complement to other noninvasive

***Address for Correspondence:** *Frederick H. Silver, Department of Pathology and Laboratory Medicine, Robert Wood Johnson Medical School, Rutgers, the State University of New Jersey, New Brunswick, NJ 08854, USA, Tel: +16104282173; E-mail: silverfr@rutgers.edu, fhsilverfh@yahoo.com*

Received: 19 November, 2024, Manuscript No. jcst-24-152914; **Editor assigned:** 21 November, 2024, PreQC No. P-152914; **Reviewed:** 02 December, 2024, QC No. Q-152914; **Revised:** 07 December, 2024, Manuscript No. R-152914; **Published:** 14 December, 2024, DOI: 10.37421/1948-5956.2024.16.678

imaging tools such as dermoscopy, high-frequency ultrasound, and confocal laser scanning microscopy [17]. While OCT images alone are useful for visual interpretation of skin lesions, additional quantitative information is contained in the images such pixel intensity differences between different skin lesions [18]. Clinical applications of OCT include detection of nonmelanoma skin cancer and evaluation of therapy for inflammatory and connective tissue diseases [19,20]. It also has been reported to be used to evaluate malignant melanomas, basal cell, and squamous cell carcinomas [19,20]. OCT imaging has the potential to serve as an objective, non-invasive measure of disease progression for use in both research trials and clinical practice [21]. The purpose of this paper is to present pilot quantitative pixel intensity *vs*. depth data and machine learning results obtained from OCT images of melanomas and SKs. Our results show that this information can be used to help noninvasively screen to differentiate between SKs and melanomas.

Methods

OCT image collection and machine learning studies

Skin lesions images both *in vivo* and as well as biopsies of suspected skin cancers were collected using an OQ Labscope 2.0 as described previously operating at a wavelength of 840 nm [18-21]. All images were made as part of IRB approved clinical studies of 26 melanomas, 22 seborrheic keratoses, and 48 samples of normal skin at both Summit Health and Robert Wood Johnson Medical School. Raw image OCT data were collected and processed using MATLAB software and image J [21]. All OCT images were scanned through the lesion cross-section parallel to the surface to create pixel intensity *vs*. depth profiles as reported previously [21]. The following quantitative parameters were collected for each sample tested and were used in machine learning studies to differentiate between different skin samples. (a) The pixel intensity across the sample parallel to the lesion surface as a function of depth; (b) the width of the pixel of intensity plots at the lesion surface; (c) the width at the half height; (d) depth at the half height (e); the maximum pixel intensity; and (f) the thickness of the image were tabulated. OCT images were color-coded for visual observation based on the pixel intensity to enhance image details for visual analysis [18-21].

Machine learning studies

To analyse the skin samples, a pixel intensity profile was obtained from Optical Coherence Tomography (OCT) images as described above. The profile was generated by tracing the surface of the skin and calculating the mean pixel intensity at each depth. From this, the maximum pixel intensity was determined, and the "half-maximum" value was calculated as half of this maximum intensity. The "half-width," representing the depth, at which the pixel intensity dropped to half of its maximum value, was also measured. Additionally, the thickness of each OCT image was included as a parameter. A comprehensive dataset was then compiled, consisting of all extracted parameters. This dataset was then used as input to a logistic regression model. A total of 22 samples of SK; 26 samples of melanoma, and 48 samples of normal skin were used. 70% of the data was used to train the model, whereas 30% was used for testing the model. The samples were characterized by a dermatopathologist after processing for pathologic analysis as part of routine clinical testing.

The model's performance was evaluated constructing a confusion matrix to calculate its sensitivity and specificity. By the following formulae were then applied to derive these metrics.

$$Sensitivity = \frac{a}{a+c}$$

$$Specificity = \frac{b}{b+d}$$

True Positive (a)	False Negative (b)
False Positive (c)	True Negative (d)

OCT images were color-coded for visual observation based on the pixel intensity to enhance image details for visual analysis [18-21]. Each pixel value in the grayscale OCT images was further evaluated by assigning a unique combination of R-G-B values using the Look up Table (Table 1). By application of digital image processing algorithms on the color-coded OCT image, the images are split into green, blue, and red channels based on the distribution of pixel intensities. A combination of green, blue, and red colors in varying intensities produce all the colors in the color-coded image; the image processing algorithms map the green, blue, and red, components of each pixel. By breaking up the total image into differences in pixel intensity distribution at each point, it is possible to examine differences in scattering potential of the different layers of skin and skin lesions. Skin layers containing large aggregates greater than about one tenth of the light wavelength will forward scatter light and appear to have lower surface pixel intensities compared to normal skin. If large lesion aggregates exist, whether they be due to melanin particles, cell aggregates, or large diameter collagen fibers, they may limit light reflection and result in a decrease in OCT image brightness of the epidermis and papillary dermis.

Table 1. Fire Lookup Table (LUT) for color coding the OCT images.

Greyscale Value	Red Channel	Green Channel	Blue Channel
0	0	0	0
50	104	0	221
100	201	7	78
150	255	129	0
200	255	219	0
255	255	255	255

Results

Color-coded OCT images

When the skin lesions were imaged in the OCT scanning mode, a variety of subsurface features were observed including the stratum corneum, basal epithelium, and the papillary dermis. While individual cell details are not visible *via* conventional OCT, the stratum corneum, basal epithelium, rete ridges, and papillary dermis are seen as described previously [21] (Figure 1A). These layers are easier to observe when the OCT image is color-coded based on the pixel intensity using NIH image J software. Figure 1 shows typical color-coded OCT images of normal skin (A), seborrheic keratosis (B) and melanoma (C). Note normal skin contains an undulating well defined stratum

corneum and rete ridges while typically SK has regions of thickened stratum corneum. Melanoma typically exhibits a broken stratum corneum. Figures 2-4 show images created from the different pixel intensities generated using Table 1. The green, blue, and red channels that are derived from the images shown in at low (Figure 2), medium (Figure 3), and high pixel (Figure 4) intensity. Note the green channel for normal skin and SK are easily seen while that for

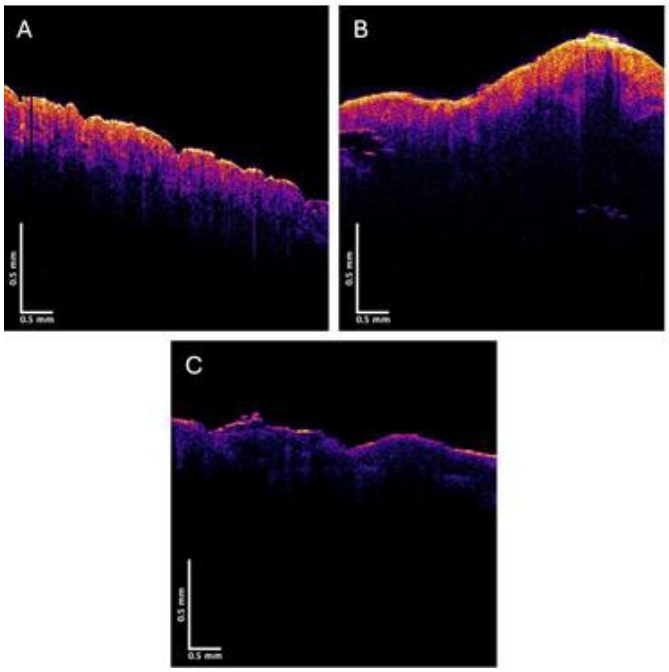

Figure 1. Color-coded OCT images of normal skin **(A)**, Seborrheic keratosis **(B)** and melanoma **(C)** generated by superimposing green, blue, and red pixel intensities on the gray scale image. Note normal skin has a well-defined stratum corneum (yellow), while SK has an enhanced stratum corneum while the stratum corneum for MEL is discontinuous.

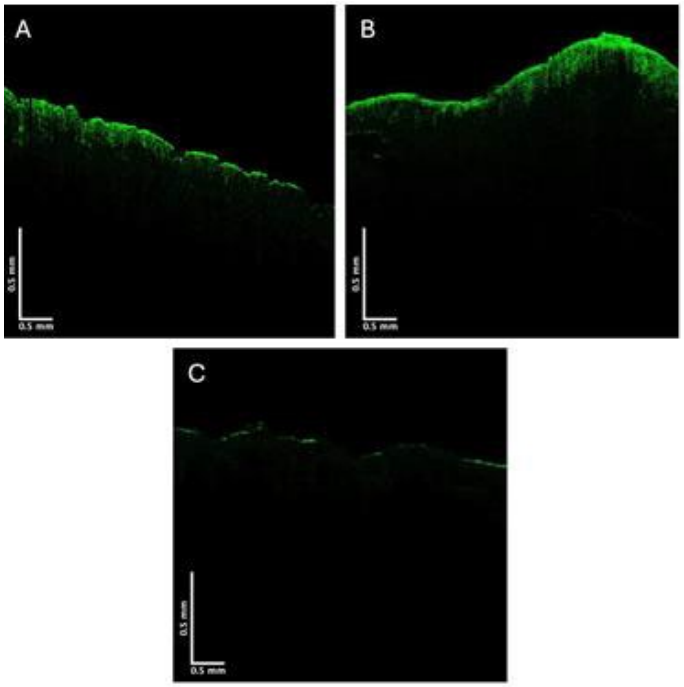

Figure 2. Typical green channel color-coded OCT low pixel intensity measurements for normal skin **(A)**, seborrheic keratosis **(B)** and melanoma **(C)** obtained using the data in Table 1. Note the green channel images for melanoma have a lower pixel intensity compared to normal skin and SK.

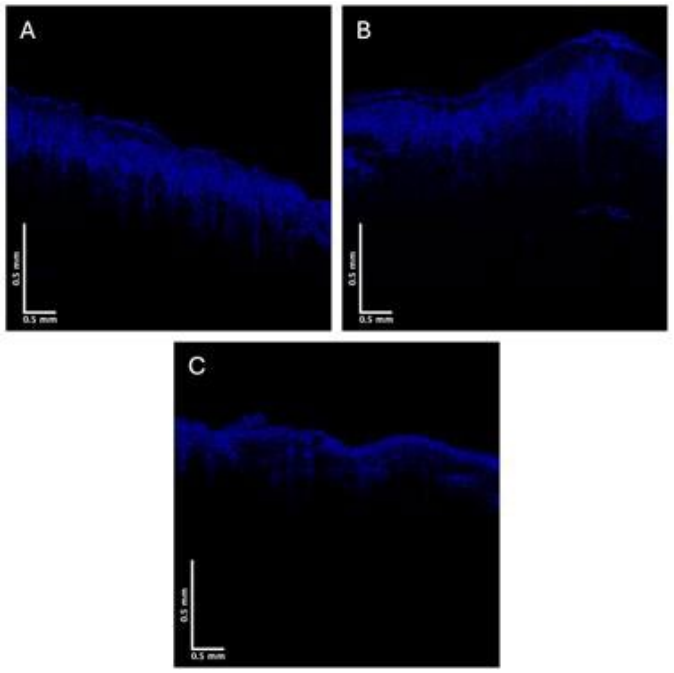

Figure 3. Typical blue channel (medium pixel intensity) color-coded OCT images for normal skin **(A)**, SK **(B)** and melanoma **(C)** obtained using lookup Table 1. Note blue channel image for melanoma appears different than for SK and Normal skin.

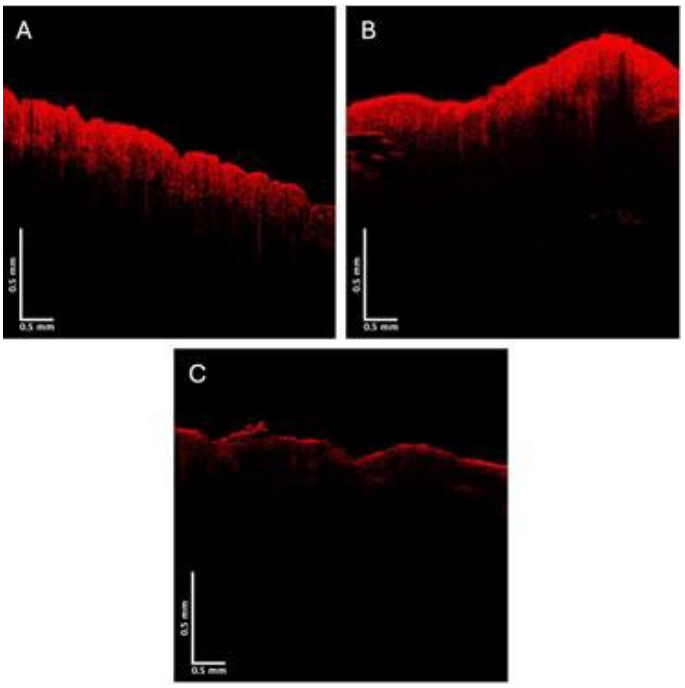

Figure 4. Typical red channel OCT images (high pixel intensity measurements) for normal skin **(A)**, SK **(B)** and melanoma **(C)**. Note red channel image of MEL shows less pixel intensity than either normal skin or SK.

MEL it is almost nonexistent in comparison. Figures 5-7 show plots of pixel intensity *vs.* depth created by scanning the images in Figures 2-4. It is noted that MEL images exhibit lower surface pixel intensities in the green channel image compared to normal skin possibly due to the formation of large melanin aggregates, cell aggregates and fibrotic collagen that scatter light towards the papillary dermis [21].

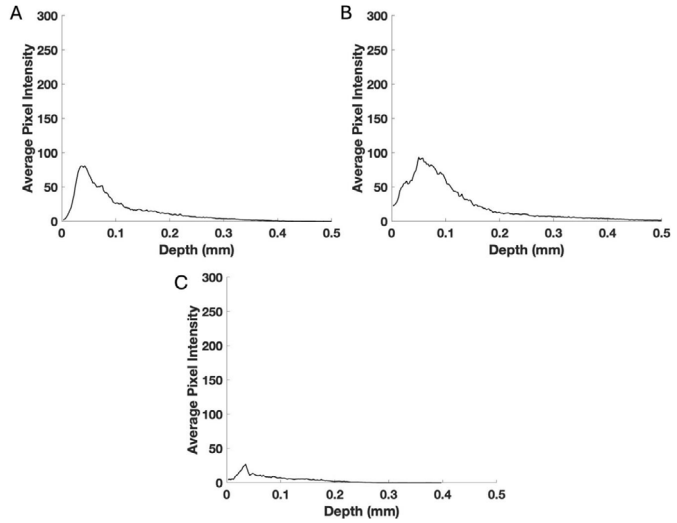

Figure 5. Typical pixel intensity versus depth scans for the green channel images seen in Figure 2 for normal skin **(A)**, SK **(B)** and melanoma **(B)**. Note the difference in scans for SK and Melanoma compared to normal skin.

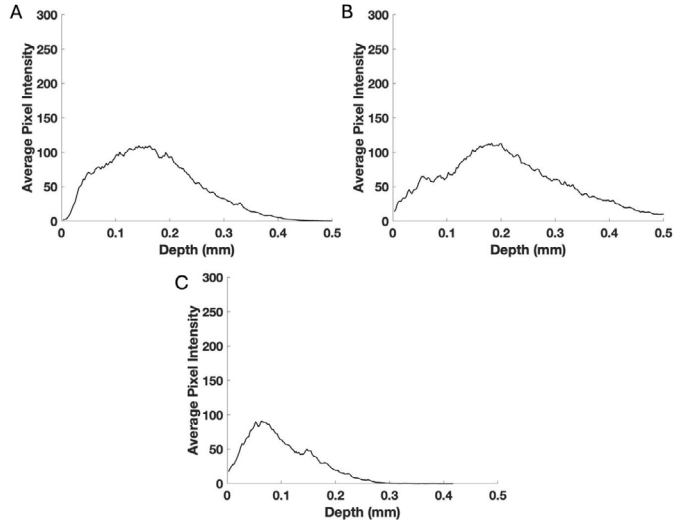

Figure 6. Typical blue channel pixel intensity versus depth plots obtained from *Figure 3* for normal skin **(A)**, SK **(B)** and melanoma **(C)** derived from images seen in Figure 3. Note the maximum pixel intensity is similar for all samples tested; however, the width of the peaks differs for melanoma, SK, and normal skin.

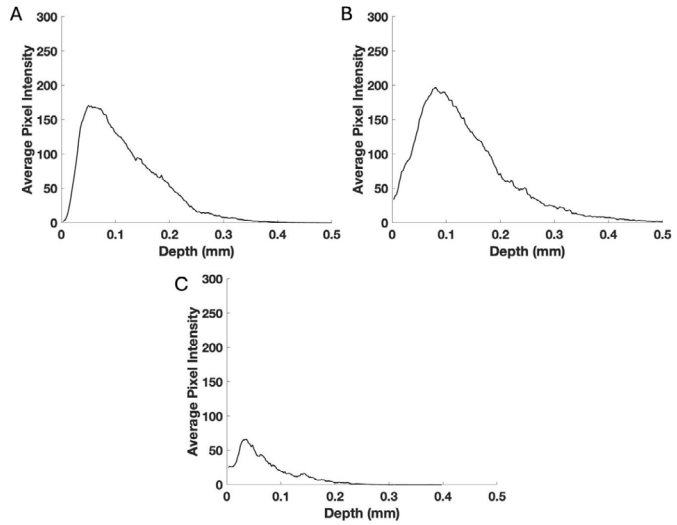

Figure 7. Typical red channel pixel intensity plots for normal skin **(A)**, SK **(B)** and Melanoma**(C)**. Note the similarity in the maximum pixel intensity for normal skin and SK but not for melanoma MEL. Note the maximum pixel intensity of MEL is much lower than the other samples studied.

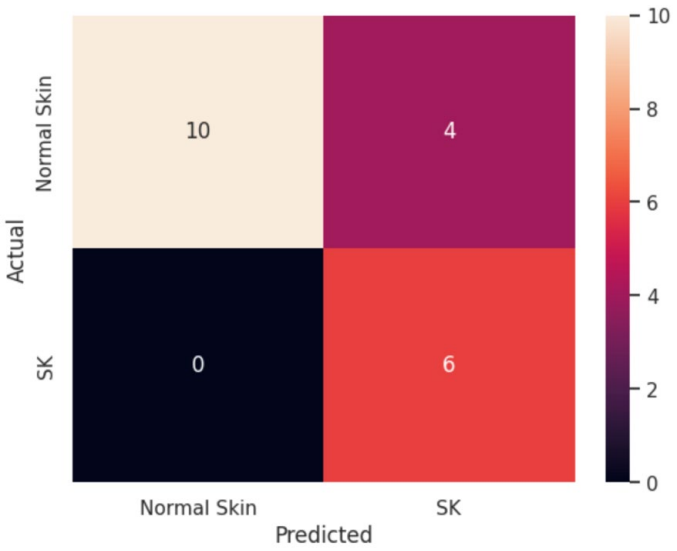

Specificity	100%
Sensitivity	60%

Figure 8. Confusion matrix for normal skin and SK and the specificity and sensitivity of differentiating between normal skin and SK. Note normal skin can be differentiated from SK with 100% specificity. However, the sensitivity is only 60% indicating that some normal skin samples are predicted to be SK.

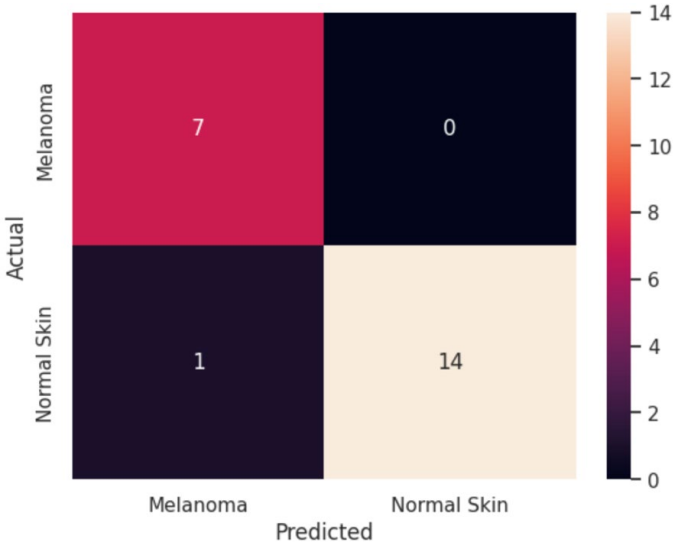

Specificity	87.5%
Sensitivity	100%

Figure 9. Confusion matrix differentiating between normal skin and melanoma as well as the specificity and sensitivity. Note normal skin can be differentiated from melanoma with 87.5% specificity and 100% sensitivity.

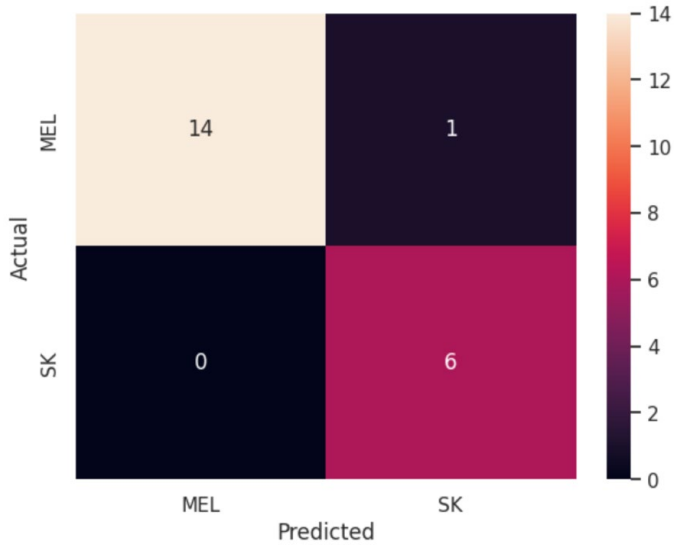

Specificity	86%
Sensitivity	100%

Figure 10. Confusion matrix for differentiating between SK and melanoma as well as the specificity and sensitivity of the analysis. Note melanoma can be differentiated from SK with a sensitivity of 100% and specificity of 86%.

Discussion

When light impinges on the surface of the skin only a small fraction is reflected, regardless of the incident wavelength, pigmentation, or structure [22-24]. Most of the light contacting the skin surface penetrates through the stratum corneum and enters the epidermis and dermis [24]. Epidermal scattering of light entering the skin can be greater due to the presence of large melanin particles in the epidermis [22-24]. In normal skin little light is scattered due to the small size of the melanin particles [22-24]. Mia scattering in the forward direction (along the beam direction) occurs when the diameters of the scattering elements such as melanin particles are similar to the light wavelength [22-24]. The primary chromophores in skin are melanin, heme, and opsin photoreceptors. They provide little absorption of light between light wavelengths of 600 and 1300 nm [22-24]. If scattering measurements are made at wavelengths above 600 nm, little light is absorbed by skin chromophores. Therefore, infrared light used in this study at 840 nm to examine the structure of skin results in images that characterize the reflection of light from substructural elements primarily in the epidermis and papillary dermis. Breaking down the pixel intensity as a function of depth provides quantitative information on the location of any large aggregates of melanin particles and cells in the skin. Our pilot machine learning results based on the pixel intensity *vs.* depth measurements can be used to differentiate between SK and melanoma with a high sensitivity (100%) a slightly lower specificity (86%). Similar results were found for differentiating normal skin and melanoma (100% and 87.5%). The ability to differentiate between normal skin and SK was somewhat less effective with a sensitivity of only 60% and a specificity of 100%. These results indicate that use of OCT images and pixel intensity *vs.* depth measurements can be used to distinguish between melanoma and SK but are less effective in distinguishing between SK and normal skin.

Two forms of melanin exist in skin, eumelanin and pheomelanin [25,26]. Since the beneficial effects of melanin are attributed mainly to eumelanin, it has been proposed that skin cancer is due to the reduced amount of eumelanin in the skin and increased formation of pheomelanin [26]. In this pilot study, we have suggested that the differences in SK and melanoma can be evaluated based on the forward scattering light into the lower layers of the lesions typically associated with a reduced green scale image and a reduced pixel intensity at all depths within the lesion. While research has been reported using OCT to evaluate pathological ocular and skin conditions [14,15] additional information can be gleaned beyond just examining OCT images by eye. It is possible to quantitatively evaluate differences among skin lesions by producing pixel intensity *vs.* depth plots and then breaking them down by pixel intensity measurements [17-20]. Since there is little absorption by skin chromophores at light wavelengths between 600 and 1000 nm the differences observed in this pilot study are likely to be a result of scattering differences especially by melanomas. The enhanced scattering by SK and normal skin in the green channel may be due to the difference in the size and amount of melanin scattering elements compared to melanoma. Recently it was reported that melanin stacking differences may occur in highly pigmented melanomas based on OCT images and vibrational optical coherence tomography measurements [20].

While melanoma cells are the original source of melanin, keratinocytes, and melanophages also contribute to the tumor color because they contain melanin obtained from melanoma cells [24-26]. Scattering from melanosomes and fragmented melanosomes is of particular significance. Melanins are particularly good scatterers since they have very high refractive indices and are contained within melanosome particles of dimensions varying within the range up to 1000 nm [26]. Quantitatively analyzing the green, blue, and red channel images that are derived from OCT scans of skin may allow for the noninvasive screening of patients that may have early melanoma lesions. The mechanism by which pheomelanin promotes carcinogenesis may be related to increased reactive oxygen species production that is associated with its synthesis [26]. If eumelanin forms large particles in melanoma, then this would explain why the green channel image for melanoma is weaker than the other lesions tested. While this is a pilot study, it suggests that additional work is needed to further support the use of sensitivity and specificity for differentiating SK and melanoma noninvasively based on OCT images. The use of OCT in conjunction with visual inspection and dermoscopy may provide more in-depth screening for melanomas. The ability to collect OCT lesion data noninvasively alllows screening of patients with skin lesions remotely by general practitioners and allied health professionals in areas where dermatologist visits are difficult to schedule.

Conclusion

We have studied the pixel intensity of OCT images of normal skin, SK, and melanoma by breaking OCT images into low (green), medium (blue), and high (red) pixel intensity *vs.* depth images and plots. While normal skin and SK are characterized by higher green scale pixel intensity *vs.* depth plots, melanoma has a lower green scale pixel intensity *vs.* depth plot. Melanoma also has lower red scale pixel intensity *vs.* depth plot compared to SK and normal skin. Our results show decreased pixel intensity of the superficial epidermis occurs in melanoma that is likely due to formation of melanin aggregates that approach the wavelength of light in size. The decreased pixel intensity of melanoma appears to be a result of increased amounts of large melanin particles in melanocytes and keratinocytes. The specificity and sensitivity of differentiating normal skin and SK from melanoma based on pixel intensity *vs.* depth measurements ranges from 86% to 100%, respectively. These results suggest that quantitative evaluation of color-coded OCT images may be useful in differentiating SKs from melanomas and can be done remotely using an OCT device run over the internet.

Acknowledgement

None.

Conflict of Interest

None.

References

1. Long, Georgina V., Susan M. Swetter, Alexander M. Menzies and Jeffrey E. Gershenwald, et al. "Cutaneous melanoma." *The Lancet* 402 (2023): 485-502.
2. Bucchi, Lauro, Silvia Mancini, Federica Zamagni and Emanuele Crocetti, et al. "Patient presentation, skin biopsy utilization and cutaneous malignant melanoma incidence and mortality in northern Italy: Trends and correlations." *J Eur Acad Dermatol Venereol* 37 (2023): 293-302.
3. Whiteman, David C., Adele C. Green and Catherine M. Olsen. "The growing burden of invasive melanoma: Projections of incidence rates and numbers of new cases in six susceptible populations through 2031." *J Invest Dermatol* 136 (2016): 1161-1171.
4. Adler, Nikki R., John W. Kelly, Pascale Guitera and Scott W. Menzies, et al. "Methods of melanoma detection and of skin monitoring for individuals at high risk of melanoma: New Australian clinical practice." *Med J Aust* 210 (2019): 41-47.
5. Leonardi, Giulia C., Luca Falzone, Rossella Salemi and Antonino Zanghì, et al. "Cutaneous melanoma: From pathogenesis to therapy." *Int J Oncol* 52 (2018): 1071-1080.
6. Davis, Lauren E., Sara C. Shalin and Alan J. Tackett. "Current state of melanoma diagnosis and treatment." *Cancer Biol Ther* 20 (2019): 1366-1379.
7. Arnold, Melina, Deependra Singh, Mathieu Laversanne and Jerome Vignat, et al. "Global burden of cutaneous melanoma in 2020 and projections to 2040." *JAMA Dermatol* 158 (2022): 495-503.
8. Bucchi, Lauro, Silvia Mancini, Federica Zamagni and Emanuele Crocetti, et al. "Patient presentation, skin biopsy utilization and cutaneous malignant melanoma incidence and mortality in northern Italy: Trends and correlations." *J Eur Acad Dermatol Venereol* 37 (2023): 293-302.
9. Gershenwald, Jeffrey E. "Mitotic rate in primary cutaneous melanoma: Cell division matters." *Cancer* 129 (2023): 2290-2293.
10. Yeatman, J. M., M. Kilkenny and Robin Marks. "The prevalence of seborrhoeic keratosis in an Australian population: Does exposure to sunlight play a part in their frequency?." *Br J Dermatol 137* (1997): 411-414.
11. Ye, Qian, Ke-Jun Chen, Meng Jia and Sheng Fang. "Clinical and histopathological characteristics of tumors arising in seborrheic keratosis: A study of 1365 cases." *Ther Clin Risk Manag* (2021): 1135-1143.
12. Bozsányi, Szabolcs, Klára Farkas, András Bánvölgyi and Kende Lőrincz, et al. "Quantitative multispectral imaging differentiates melanoma from seborrheic keratosis." *Diagnostics* 11 (2021): 1315.
13. Park, Eun Soo. "Skin-layer analysis using Optical Coherence Tomography (OCT)." *Med Lasers* 3 (2014): 1-4.
14. Olsen, Jonas, Jon Holmes and Gregor BE Jemec. "Advances in optical coherence tomography in dermatology-a review." *J Biomed Opt 23* (2018): 040901-040901.
15. Zeppieri, Marco, Stefania Marsili, Ehimare Samuel Enaholo and Ayishetu Oshoke Shuaibu, et al. "Optical Coherence Tomography (OCT): A brief look at the uses and technological evolution of ophthalmology." *Medicina* 59 (2023): 2114.
16. Wan, B., Clarisse Ganier, X. Du-Harpur and N. Harun, et al. "Applications and future directions for optical coherence tomography in dermatology." *Br J Dermatol* 184 (2021): 1014-1022.
17. Mogensen, Mette, Lars Thrane, Thomas M. Jørgensen and Peter E. Andersen, et al. "OCT imaging of skin cancer and other dermatological diseases." *J Biophotonics* 2 (2009): 442-451.
18. Silver, Frederick H., Tanmay Deshmukh, Kelly Ritter and Hari Nadiminti. "Differences between edges and centers of melanomas using vibrational optical coherence tomography: The effects of critical lesion size."
19. Babalola, Olubukola, Andrew Mamalis, Hadar Lev-Tov and Jared Jagdeo. "Optical Coherence Tomography (OCT) of collagen in normal skin and skin fibrosis." *Arch Dermatol Res* 306 (2014): 1-9.
20. Silver, Frederick H., Tanmay Deshmukh, Hari Nadiminti and Isabella Tan. "Melanin stacking differences in pigmented and non-pigmented melanomas: Quantitative differentiation between pigmented and non-pigmented melanomas based on light-scattering properties." *Life* 13 (2023): 1004.
21. Lister, Tom, Philip A. Wright and Paul H. Chappell. "Optical properties of human skin." *J Biomed Opt* 17 (2012): 090901-090901.
22. Jacques, Steven L. "Optical properties of biological tissues: A review." *Phys Med Biol* 58 (2013): R37.
23. Yang, Marjorie F., Valery V. Tuchin and Anna N. Yaroslavsky. "Principles of light-skin interactions." *Light-Based Therapies for Skin of Color* (2009): 1-44.
24. Diffey, Brian L. "What is light?." Photodermatology, Photoimmunology & Photomedicine 18 (2002): 68-74.
25. Zonios, George, Aikaterini Dimou, Ioannis Bassukas and Dimitrios Galaris, et al. "Melanin absorption spectroscopy: New method for noninvasive skin investigation and melanoma detection." *J Biomed Opt* 13 (2008): 014017-014017.
26. Nasti, Tahseen H. and Laura Timares. "MC 1R, eumelanin and pheomelanin: Their role in determining the susceptibility to skin cancer." *Photochem Photobiol* 91 (2015): 188-200.

How to cite this article: Silver, Frederick H., Tanmay Deshmukh, Aanal Patel and Hari Nadaminti. "Use of Pixel Intensity Measurements Derived from OCT Images to Differentiate Between Seborrheic Keratosis and Melanomas: A Pilot Study." *J Cancer Sci Ther* 16 (2024): 678.